Cite this paper: Chen, X.-M.; Chen, Y.; Liu, Y. *Chin. J. Chem.* **2018**, *36*, 526—530.

Concise Report

DOI: 10.1002/cjoc.201800063

Multiple-Stimuli Responsive and Tunable Luminescent Supramolecular Assembly by Oligo(*p*-phenylvinylene) and Surfactant

Xu-Man Chen,[a] Yong Chen,[a,b] and Yu Liu*[a,b]

ABSTRACT Achieving multicolor photoluminescence under multiple stimuli response based on a single fluorescent compound remains a great challenge. Herein, we report a novel multicolor fluorescent supramolecular assembly, which was constructed from surfactant sodium dodecyl sulfate (SLS) and fluorescent compound **1** bearing a rigid symmetrical acceptor–donor–acceptor structure. The luminescence property of **1**/SLS assembly showed the multiple stimuli response towards temperature, cyclodextrin complexation and UV light irradiation, exhibiting the tunable emission wavelengths from 490 nm to 590 nm and the multicolor photoluminescence including cyan, green, yellow and orange. Furthermore, this assembly could be used in light writing owing to the fast fluorescence change within 15 s. These results could provide a convenient and useful method for fabricating smart tunable photoluminescent materials.

KEYWORDS tunable photoluminescence, supramolecular assembly, multiple stimuli response, oligo(*p*-phenylvinylene), surfactant

Introduction

Supramolecular self-assembly constructed via noncovalent methods is widely utilized for fabricating various smart nanomaterials.[1] Among them, the tunable photoluminescent material for displaying multicolor induced by external stimuli is one of the most important applications[2] and widely used as fluorescent probes, sensors, imaging agents, logic gates and molecular machines.[3] However, the preparation of such functional luminescent materials usually requires the multi-stepped organic synthesis and high cost,[4] the development of water-soluble organic luminescence materials is still a challenge. Recently, supramolecular assembly becomes a rational way to construct smart photo-functional nanomaterials.[5] In this way, chromophores can be included into assemblies through noncovalent interactions, such as hydrophobic interactions, π-π stacking, host-guest complexation, electrostatic interactions and hydrogen bonding, to change the conformation, arrangement, environment and thus to gain novel optical properties. In addition, the morphological, photophysical and catalytic properties of supramolecular assemblies are also adjustable through various stimuli response.[6]

On the other hand, oligo(*p*-phenylvinylene) (OPV) dyes are widely applied in light-harvesting systems and supramolecular assemblies.[7] Recently, Ni and coworkers reported tunable luminescent materials in aqueous solution based on host-guest interactions between cucurbit[8]uril and OPV.[8] Tian *et al*. constructed tunable luminescent materials from a dual-emission luminescent molecule and γ-cyclodextrin.[9] Herein, we synthesized an OPV molecule **1** (Scheme 1) bearing the *p*-biphenylvinylene unit as the electron donor and the pyridinium units as the electron acceptors, which can aggregate with the surfactant sodium dodecyl sulfate (SLS) to form supramolecular assembly with tunable fluorescence emission wavelengths from 490 nm to 590 nm. Furthermore, the fluorescence of such assembly can be tuned by multiple stimuli including temperature, addition of cyclodextrin, and UV light irradiation. Significantly, this assembly can be used in light writing due to the fast fluorescence change within 15 s.

Scheme 1 Schematic illustration of multiple stimuli responsive supramolecular assemblies for tunable photoluminescence

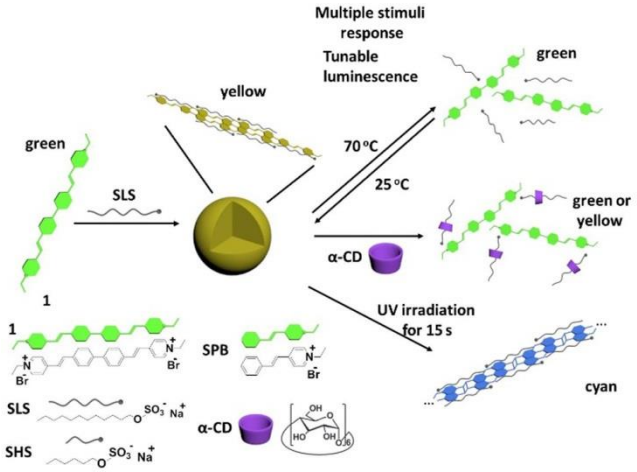

Results and Discussion

Characterization of 1/SLS supramolecular assembly. Firstly, the intermolecular association between **1** and SLS was investigated. In the presence of SLS, all of ^{1}H NMR signals assigned to protons of **1** moved downfield and broadened, probably due to the restriction of intramolecular rotation (Figure S1).[10] 2D NOESY spectra also gave the strong nuclear overhauser effect (NOE) signals between $H_{a,b,c,d,e,f}$ protons of **1** and $H_{1,2,3,4,5}$ protons of SLS (Figure 1a). In UV-Vis spectra, with the addition of SLS, the absorbance maximum of **1** at 395 nm decreased, accompanied by the appearance of a new absorbance maximum at 460 nm (Figure S2a). Moreover, Job's plot gave a 1 : 2 association stoichiometry between **1** and SLS (Figure S3), referring to two possible association modes of **1**/SLS system. One is the head-to-tail interlaced orientation with a *n* : 2*n* stoichiometry (Figure 1b); the other is face-to-face paralleled orientation with a 1 : 2 stoichiometry (Figure 1c). Owing to the NOE correlations of H_g protons of **1** with $H_{e,f}$ protons of **1** as well as SLS protons in 2D NOESY spectra, we deduced that the **1**/SLS system should adopt a head-to-tail aggregation motif, which was further verified by the red shift of UV-Vis absorbance due to the interlaced J-aggregation of aggregation motif (Figure S2a).[11] From the UV-Vis titration curves, the association constants (K_a) of **1**/SLS system were calculated as K_{a1} = (1.31 ± 0.96) × 10^6 M^{-1} and K_{a2} = (1.32 ± 0.96) × 10^5 M^{-1} by using a nonlinear least-squares curve-fitting method (Figure S2b). In the control experiment, no appreciable changes could be observed

[a] College of Chemistry, State Key Laboratory of Elemento-Organic Chemistry, Nankai University, Tianjin 300071, China
[b] Collaborative Innovation Center of Chemical Science and Engineering (Tianjin), Nankai University, Tianjin 300071, China
*E-mail: yuliu@nankai.edu.cn

when adding a reference surfactant SHS to the solution of **1** instead of SLS. Similarly, the addition of SLS to a solution of SPB, a reference compound bearing half of a unit of **1**, also led to nearly no UV-Vis absorbance changes (Figure S4).

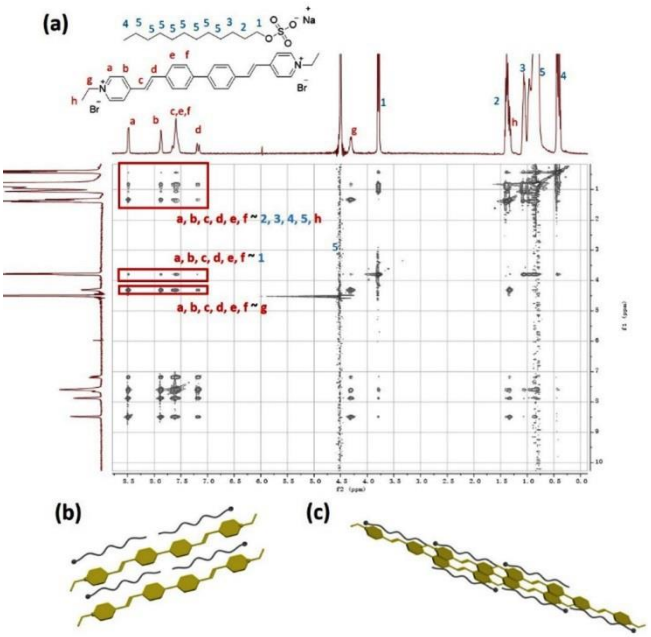

Figure 1 (a) 2D ROESY NMR spectrum of **1**/SLS system ([**1**] = 2 mM, [SLS] = 8 mM) in D_2O at 25 °C. Schematic illustration of (b) face-to-face paralleled orientation with 1 : 2 and (c) head-to-tail interlaced orientation with *n* : 2*n* aggregation motif.

The aggregation behavior and morphological information of **1**/SLS system were also investigated. As seen in Figure S5, the **1**/SLS showed the obvious Tyndall effect, indicating the formation of large aggregates in solution, while neither free **1** nor free SLS exhibited the Tyndall effect under the same condition. The critical aggregation concentration (CAC) of **1**/SLS system was determined by measuring the optical transmittance of one component at a fixed concentration with varying concentrations of the other component. As shown in Figures S6 and 2a, when the concentrations of **1** varied from 0 to 0.028 mM, the optical transmittances of SLS (0.056 mM) at 550 nm exhibit the different linear variations, and an inflection point at 0.0063 mM was observed on the plot of optical transmittance at 550 nm versus the concentration of **1**, referring to an aggregation-induced CAC value of **1** as 0.0063 mM in the presence of SLS. The preferable mixing ratio between **1** and SLS was also measured. With the concentration of SLS ranging from 0 to 0.2 mM in a solution of **1** (0.02 mM), the optical transmittances at 550 nm exhibited a sharp decrease before the concentration of SLS reached 0.056 mM, and then gradually recovered to the original level by continuously raising concentration of SLS to 0.2 mM (Figures S7 and 2b). Accordingly, the preferable mixing ratio of **1**/SLS system was measured as 0.02 mM **1**/0.056 mM SLS. In Figure 2c, the dynamic light scattering (DLS) measurements gave the average hydrodynamic diameter of **1**/SLS system as 383 nm at a scattering angle of 90°. Furthermore, the transmission electron microscopy (TEM) and scanning electron microscopy (SEM) images of **1**/SLS system both showed many spherical nanoparticles with an average diameter of *ca*. 400 nm (Figures 2d and S8), which was basically consistent with the corresponding value measured by DLS.

Photophysical property of 1/SLS supramolecular assembly. Without SLS, the fluorescence emission and excitation wavelengths of **1** were 515 nm and 410 nm (Figure S9), but gradually

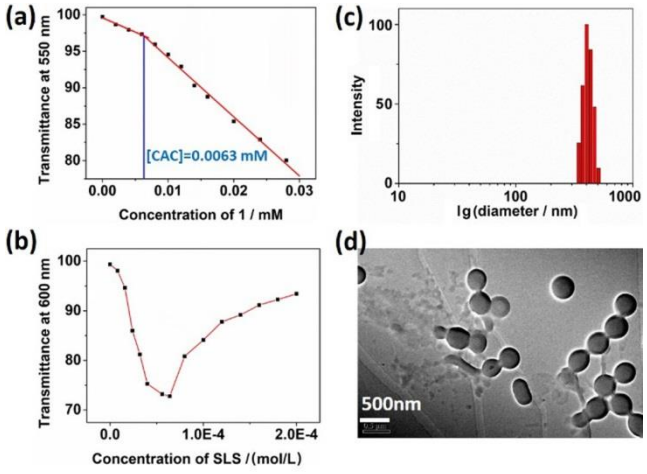

Figure 2 (a) Dependence of optical transmittance at 550 nm *versus* the concentration of **1** in SLS (0.056 mM). (b) Dependence of optical transmittance at 600 nm on the SLS concentration in the presence of **1** (0.02 mM). (c) DLS data and (d) TEM image of **1**/SLS nanoparticles ([**1**] = 0.02 mM, [SLS] = 0.056 mM).

shifted to 590 nm and 460 nm, respectively after the gradual addition of SLS. Therefore, we could achieve the multicolor emissions by varying the concentration of SLS added to the solution of **1** (Figures 3a, 3b and 4a). It is noteworthy that the color of emissions changed nonlinearly, indicating that the fluorescence was not the simple mixture of two emission states of **1** before and after associating with SLS but underwent the multiple emission states during the process of supramolecular assembly with SLS.

Significantly, the assembly/disassembly behavior and photophysical property of assemblies could be easily adjusted by multiple stimuli. As seen in Figure S10 and Figure S11, when the temperature rising from 298 K to 343 K, the UV-Vis absorbance maximum of **1**/SLS assembly at 460 nm decreased while that at 395 nm increased, indicating the disruption of **1**/SLS assembly. However, when cooling the solution of **1**/SLS assembly back to 298 K, the UV-Vis spectrum recovered to the original shape, indicating the re-formation of assembly. The reversible assembly/disassembly progress by varying the temperature between 298 K and 343 K could be repeated for several circles (Figure S11b). Interestingly, this reversible assembly/disassembly progress was also accompanied by the obvious color changes of fluorescence emission. When excited at 410 nm, the **1**/SLS assembly emitted the orange fluorescence (emission maximum 590 nm) at 298 K but emitted the green fluorescence (emission maximum 515 nm) at 343 K (Figures 3c, 3d and 4b). However, when excited at 460 nm, the emission maximum of **1**/SLS assembly changed from 590 nm to 535 nm with the fluorescence quenching by heating the **1**/SLS solution from 298 K to 343 K (Figure S12). On the other hand, when α-cyclodextrin (α-CD) was added to the **1**/SLS solution, the emission maximum of **1**/SLS shifted from 590 nm to 520 nm when excited at 410 nm with a fluorescence color change from orange to green (Figures 3e, 3f and 4c), but remained nearly unchanged when excited at 460 nm (Figure S13). A possible reason may be that α-CD could include the alkyl chain of SLS, which weakened the hydrophobic interactions between **1** and SLS, but the electrostatic interactions of **1**/SLS remained unchanged. Furthermore, when the **1**/SLS assembly was irradiated by 395 nm UV light for 15 s, the emission maximum rapidly changed from 590 nm to 490 nm, with the fluorescence color changing from orange to yellow, green, and finally to cyan (Figures 3g, 3h and 4d). It is well documented that the C=C double bond of OPV dye can undergo four possible photoreactions under UV light irradiation: *cis-trans* isomerization, oxidation by oxygen from air, addition reaction

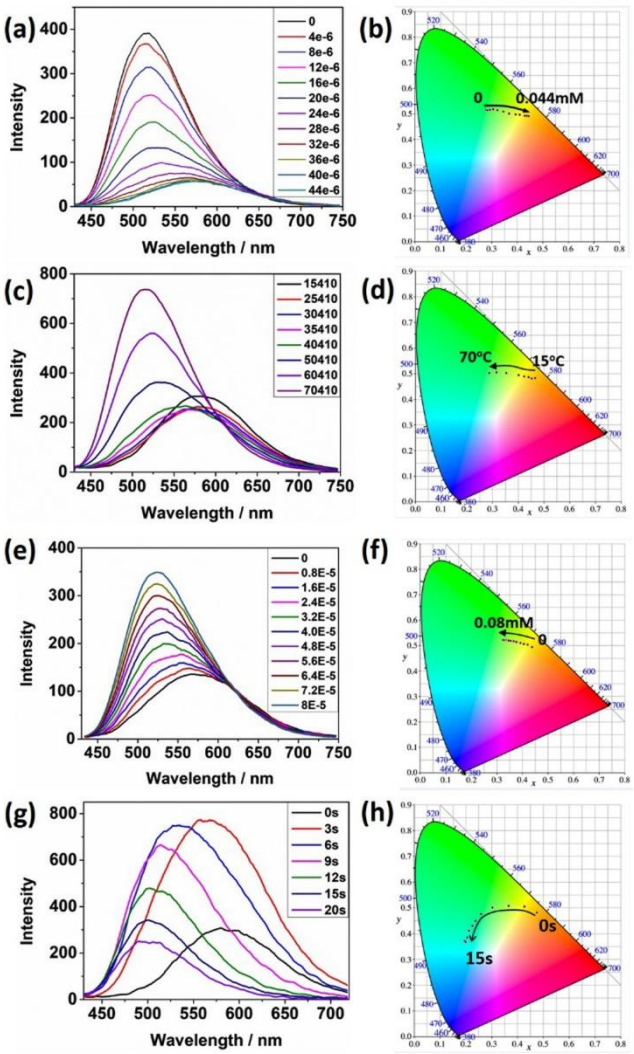

Figure 3 (a) Fluorescence spectra and (b) luminescent color in CIE 1931 chromaticity diagram of aqueous solutions containing **1** (0.02 mM) and SLS at different concentrations from 0 to 0.044 mM at 25 °C; (c) Fluorescence spectra and (d) luminescent color in CIE 1931 chromaticity diagram of aqueous **1**/SLS at various temperature from 15 °C to 70 °C (λ_{ex} = 410 nm); (e) Fluorescence spectra and (f) luminescent color in CIE 1931 chromaticity diagram of aqueous **1**/SLS with different concentrations of α-CD ranging from 0 to 0.08 mM at 25 °C (λ_{ex} = 410 nm); (g) Fluorescence spectra and (h) luminescent color in CIE 1931 chromaticity diagram of aqueous **1**/SLS under UV irradiation for different time from 0 to 20 s.([**1**] = 0.02 mM, [SLS] = 0.056 mM in figure (c, d, e, f, g, h)).

with water, or cycloaddition reaction.[12] To investigate the possible reaction mechanism in the present case, ^{1}H NMR, mass spectra, 2D NOESY, UV-Vis and TEM experiments were performed. In the ^{1}H NMR spectra, the integral amounts of protons of **1** remained nearly unchanged after the UV irradiation, indicating that no addition reaction occurred between **1** and water (Figure S14). The mass spectra showed that the molecular ion peak of **1** also remained unchanged after the UV irradiation (Figure S15). Meanwhile, the UV-Vis absorbance of **1**/SLS under the UV irradiation after the removal of oxygen was found very similar to that in air (Figure S16). These phenomena jointly indicated that **1** was not oxidized by oxygen in air. In addition, the UV-Vis absorbance of **1**/SLS at 400—500 nm, which was assigned to the intramolecular charge transfer (ICT), greatly decreased under the UV irradiation. Therefore, we deduced that the cycloaddition reaction between the C=C double bonds, rather than the *cis-trans* isomerization, should occur under the UV irradiation.

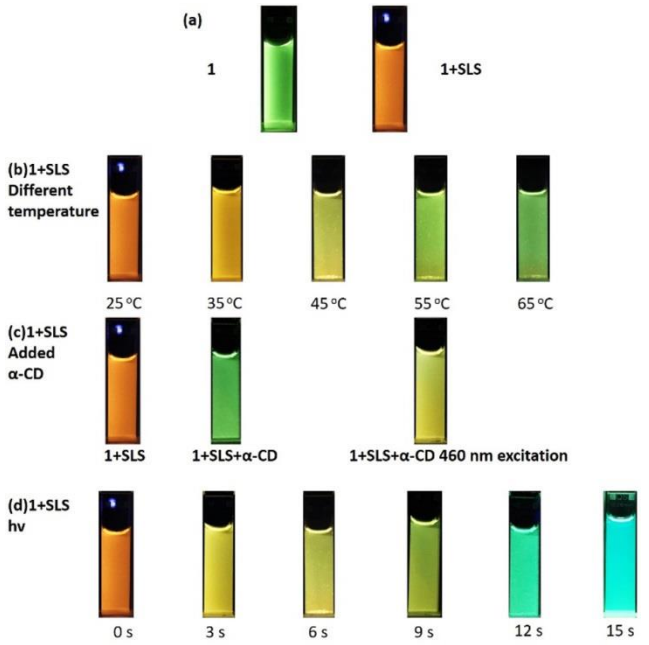

Figure 4 Photos of fluorescence of (a) aqueous **1** and **1**/SLS assemblies; (b) **1**/SLS assemblies under different temperature; (c) **1**/SLS added α-CD (0.08 mM) under different excitation; (d) **1**/SLS under 395 nm UV light irradiation for different time. All of the photos were taken under 365 nm UV lamp unless otherwise noted. ([**1**] = 0.02 mM, [SLS] = 0.056 mM).

On the other hand, there are also two possible cycloaddition reactions: one is the face-to-face cycloaddition reaction between two units of **1** (dimerization), and the other is head-to-tail interlaced cycloaddition of multiple units of **1** (oligomerization) (Figure S17). The 2D NOESY spectra of **1**/SLS after the UV irradiation showed the clear NOE correlations between $H_{g,h}$ protons and $H_{e,f}$ protons (Figure S18). Moreover, TEM images showed that the spherical **1**/SLS nanoparticles were cross-linked to network after the UV irradiation (Figure S19). These jointly demonstrated the head-to-tail interlaced cycloaddition reaction mode. By treating the photoreaction as a first-order reaction, the reaction rate of **1** was measured as k_r = (0.152 ± 0.003) s^{-1} with SLS, which was 175 times higher than the corresponding value, *i.e.* k_r = (8.67 ± 0.07) × 10^{-4} s^{-1}, without SLS (Figure S20). In a short video, the fast changes of emission color within 15 s under UV irradiation were displayed.

Benefitting from the fast change of emission color under the UV irradiation, the **1**/SLS system could be used as a photo-controlled writing board. As shown in Figures 5a and 5b, the green fluorescence of **1** turned orange after the addition of SLS. With the irradiation of UV light on the **1**/SLS solution with a shape of letter "C", the fluorescence of corresponding area rapidly turned cyan (Figure 5c). After the solution was shaken, the cyan letter "C" disappeared (Figure 5d), and this writing/erasing cycle could be repeated for at least 5 times. By the UV irradiation over the whole writing board, the **1**/SLS solution finally turned cyan (Figures S21 and 5).

Conclusions

In summary, we successfully constructed a tunable supramolecular assembly with multiple stimuli responsive properties. Such supramolecular assembly can change its emission wavelength from 490 nm to 590 nm, accompanied by the obvious changes of fluorescence colors. Owing to its fast response to stimuli such as

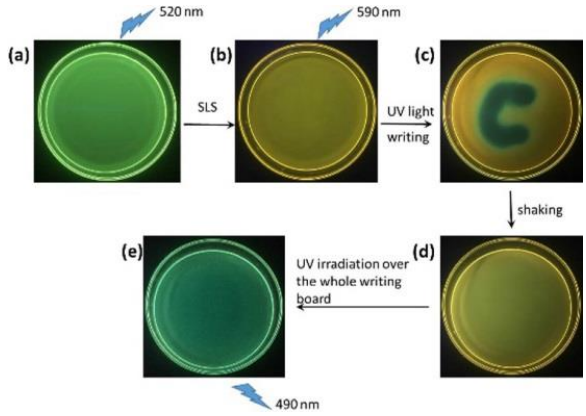

Figure 5 Luminescence of (a) **1**, (b) **1**/SLS, (c) cyan "C" written on **1**/SLS by UV light, (d) shaking the solution of (c) for recycling and (e) cyan solution which was full irradiated by UV light. ([**1**] = 0.02 mM, [SLS] = 0.056 mM).

UV irradiation, the assembly can be used as fluorescent ink by UV light writing, and such tunable luminescent supramolecular nanomaterial may possess the potential application in the field of smart nanomaterials.

Experimental

Materials

The chemical reagents were purchased from commercial resource unless noted.

Synthesis of 1

[1,1'-Biphenyl]-4,4'-dicarbaldehyde (0.210 g, 1.00 mmol) and 1-ethyl-4-methylpyridin-1-ium bromide (0.500 g, 2.47 mmol) were dissolved in 40 mL of ethanol, and the solution was heated to reflux for 12 h. Then the solution was concentrated to about 20 mL, and cooled by ice water. The formed precipitate was collected by filtration, washed by acetone, recrystallized by ethanol, and dried *in vacuo* to give **1** (0.322 g, 55.7%) as yellow powder. ^{1}H NMR (400 MHz, D_2O) δ: 8.43 (d, J = 6.4 Hz, 4H), 7.83 (d, J = 6.4 Hz, 4H), 7.67—7.48 (m, 10H), 7.09 (d, J = 16.2 Hz, 2H), 4.27 (q, J = 7.4 Hz, 4H), 1.40 (t, J = 7.3 Hz, 6H). ^{13}C NMR (101 MHz, D_2O) δ: 153.23, 142.96, 140.22, 139.85, 134.50, 128.90, 126.90, 124.03, 122.64, 55.96, 15.39. HRMS: m/z 209.1203, ([**1**]$^{2+}$, calcd for $C_{32}H_{30}N_2^{2+}$, 209.1205).

Scheme 2 Synthesis of **1**

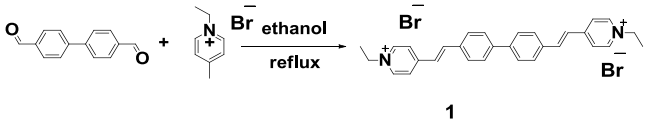

1

Measurements

NMR spectroscopy. ^{1}H NMR, ^{13}C NMR and 2D NOESY spectra were recorded on a Brucker AV400 spectrometer.

Fluorescence spectroscopy. Steady-state fluorescence spectra were recorded in a conventional quartz cell (light path 10 mm) on a Varian Cary Eclipse equipped with a Varian Cary single-cell peltier accessory to control temperature.

UV-Vis spectroscopy. UV-Vis spectra and the optical transmittance were recorded in a quartz cell (light path 10 mm) on a Shimadzu UV-3600 spectrophotometer equipped with a PTC-348WI temperature controller.

TEM microscopy. Transmission electron microscopy (TEM) images were acquired using a Tecnai 20 high-resolution transmission electron microscope operating at an accelerating voltage of 200 keV. The sample for high-resolution TEM measurements was prepared by dropping the solution onto a copper grid. The grid was then air-dried.

SEM microscopy. Scanning electron microscopy (SEM) images were obtained using a Hitachi S-3500N scanning electron microscope.

DLS spectroscopy. Solution samples were examined on a laser light scattering spectrometer (BI-200SM) equipped with a digital correlator (TurboCorr) at 636 nm at a scattering angle of 90 °. The hydrodynamic diameter (D_h) was determined by DLS experiments at 25 °C.

ESI-MS spectroscopy. Electrospray ionization mass spectra (ESI-MS) were measured by Agilent 6520 Q-TOF-MS.

Light Irradiation Experiments. The UV light irradiation experiment (λ < 395 nm) was carried out using a CEL-HXF300 14V 50W xenon lamp with cutoff filter.

Supporting Information

The supporting information for this article is available on the WWW under https://doi.org/10.1002/cjoc.201800063.

Acknowledgement

We thank NNSFC (Nos. 21432004, 21672113, 21772099 and 91527301) for financial support.

References

[1] (a) Lehn, J. M. *Science* **2002**, *295*, 2400; (b) Aida, T.; Meijer E. W.; Stupp, S. I. *Science* **2012**, *335*, 813; (c) Rybtchinski, B. *ACS Nano* **2011**, *5*, 6791; (d) Ma, X.; Tian, H. *Acc. Chem. Res.* **2014**, *47*, 1971; (e) Chen, Y.; Liu, Y. *Adv. Mater.* **2015**, *27*, 5403; (f) Würthner, F.; Kaiser, T. E.; Saha-Möller, C. R. *Angew. Chem. Int. Ed.* **2011**, *50*, 3376; (g) Thota, B. N. S.; Urner, L. H.; Haag, R. *Chem. Rev.* **2016**, *116*, 2079; (h) Li, Y. J.; Liu, T. F.; Liu, H. B.; Tian, M. Z.; Li, Y. L. *Acc. Chem. Res.* **2014**, *47*, 1186; (i) Fu, T. F.; Ao, L.; Gao, Z. C.; Zhang, X. L.; Wang, F. *Chin. Chem. Lett.* **2016**, *27*, 1147; (j) Ji, X. F.; Xia, D. Y.; Yan, X. Z.; Wang, H.; Huang, F. H. *Acta Polym. Sin.* **2017**, 9; (k) Wei, T.; Zhang, H.; Li, W.; Qu, W.; Su, J.; Lin, Q.; Zhang, Y.; Yao, H. *Chin. J. Chem.* **2017**, *35*, 1311; (l) Pan, T.; Zou, H.; Sun, H.; Liu, Y.; Liu, S.; Luo, Q.; Dong, Z.; Xu, J.; Liu, J. Q. *Chin. J. Chem.* **2017**, *35*, 871; (m) Yi, J. M.; Chen, M. H.; Xue, S. F.; Tao, Z. *Chin. J. Org. Chem.* **2016**, *36*, 653; (n) Li, W. T.; Qu, W. J.; Zhang, H. L.; Li, X.; Lin, Q.; Yao, H.; Zhang, Y. M.; Wei, T. B. *Chin. J. Org. Chem.* **2017**, *37*, 2619; (o) Bai, D.; Wang, X.; Gao, Z. Z.; Qiu, S. C.; Tao, Z.; Zhang, J. X.; Xiao, X. *Chin. J. Org. Chem.* **2017**, *37*, 2022.

[2] (a) Ding, H.; Yu, S. B.; Wei, J. S.; Xiong, H. M. *ACS Nano* **2016**, *10*, 484; (b) Zhang, J. N.; Kang, H.; Li, N.; Zhou, S. M.; Sun, H. M.; Yin, S. W.; Zhao, N.; Tang, B. Z. *Chem. Sci.* **2017**, *8*, 577; (c) Zhang, H.; Wang, X.; Liao, Q.; Xu, Z.; Li, H.; Zheng, L.; Fu, H. *Adv. Funct. Mater.* **2017**, *27*, 1604382; (d) Han, J.; You, J.; Li, X.; Duan, P.; Liu, M. *Adv. Mater.* **2017**, *29*, 1606503; (e) Zhou, Y.; Zhang, H. Y.; Zhang, Z. Y.; Liu, Y. *J. Am. Chem. Soc.* **2017**, *139*, 7168.

[3] (a) Inouye, M.; Hayashi, K.; Yonenaga, Y.; Itou, T.; Fujimoto, K.; Uchida, T. A.; Iwamura, M.; Nozaki, K. *Angew. Chem. Int. Ed.* **2014**, *53*, 14392; (b) Lu, H.; Zheng, Y.; Zhao, X.; Wang, L.; Ma, S.; Han, X.; Xu, B.; Tian, W.; Gao, H. *Angew. Chem. Int. Ed.* **2016**, *55*, 155; (c) Huo, S.; Duan, P.; Jiao, T.; Peng, Q.; Liu, M. *Angew. Chem. Int. Ed.* **2017**, *56*, 12174.

[4] (a) Figueira-Duarte, T. M.; Müllen, K. *Chem. Rev.* **2011**, *111*, 7260; (b) Frath, D.; Massue, J.; Ulrich, G.; Ziessel, R. *Angew. Chem. Int. Ed.* **2014**, *53*, 2290.

[5] (a) Yashima, E.; Ousaka, N.; Taura, D.; Shimomura, K.; Ikai, T.; Maeda, K. *Chem. Rev.* **2016**, *116*, 13752; (b) Wu, H.; Chen, Y.; Liu, Y. *Adv. Mater.* **2017**, *29*, 1605271; (c) Chen, P. Z.; Zhang, H.; Niu, L. Y.; Zhang, Y.; Chen, Y. Z.; Fu, H. B.; Yang, Q. Z. *Adv. Funct. Mater.* **2017**, *27*,

1700332; (d) Zhang, Y. M.; Zhang, X. J.; Xu, X. F.; Fu, X. N.; Hou, H. B.; Liu, Y. *J. Phys. Chem. B* **2016**, *120*, 3932; (e) Wei, T.; Zhang, H.; Li, W.; Qu, W.; Su, J.; Lin, Q.; Zhang, Y.; Yao, H. *Chin. J. Chem.* **2017**, *35*, 1311.

[6] (a) Jiang, L.; Huang, X.; Chen, D.; Yan, H.; Li, X.; Du, X. *Angew. Chem. Int. Ed.* **2017**, *56,* 2655; (b) Li, X.; Xie, Y.; Song, B.; Zhang, H. L.; Chen, H.; Cai, H.; Liu, W.; Tang, Y. *Angew. Chem. Int. Ed.* **2017**, *56,* 2689; (c) Xiong, C.; Sun, R. *Chin. J. Chem.* **2017**, *35*, 1669; (d) Li, Z.; Yang, J.; Huang, F. *Chin. J. Chem.* **2018**, *36*, 59; (e) Chen, H.; Jia, X.; Li, C. *Chin. J. Chem.* **2015**, *33*, 343; (f) Sun, Z.; Lv, F.; Cao, L.; Liu, L.; Zhang, Y.; Lu, Z. *Angew. Chem. Int. Ed.* **2015**, *54*, 7944; (g) Dong, S.; Luo, Y.; Yan, X.; Zheng, B.; Ding, X.; Yu, Y.; Ma, Z.; Zhao, Q.; Huang, F. *Angew. Chem. Int. Ed.* **2011**, *50*, 1905; (h) Pandeeswar, M.; Senanayak, S. P.; Narayan, K. S.; Govindaraju, T. *J. Am. Chem. Soc.* **2016**, *138*, 8259.

[7] (a) Ajayaghosh, A.; Praveen, V. K. *Acc. Chem. Res.* **2007**, *40*, 644; (b) Praveen, V. K.; Ranjith, C.; Bandini, E.; Ajayaghosh, A.; Armaroli, N. *Chem. Soc. Rev.* **2014**, *43*, 4222; (c) Sagara, Y.; Kubo, K.; Nakamura, T.; Tamaoki, N.; Weder, C. *Chem. Mater.* **2017**, *29*, 1273; (d) Lavrenova, A.; Balkenende, D. W. R.; Sagara, Y.; Schrettl, S.; Simon, Y. C.; Weder C. *J. Am. Chem. Soc.* **2017**, *139*, 4302.

[8] Ni, X. L.; Chen, S. Y.; Yang, Y. P.; Tao, Z. *J. Am. Chem. Soc.* **2016**, *138*, 6177.

[9] Zhang, Q. W.; Li, D. F.; Li, X.; White, P. B.; Mecinović, J.; Ma, X.; Ågren, H.; Nolte, R. J. M.; Tian, H. *J. Am. Chem. Soc.* **2016**, *138*, 13541.

[10] Hong, Y. N.; Lama, J. W. Y.; Tang, B. Z. *Chem. Commun.* **2009**, 4332.

[11] Chen, Z.; Liu, Y.; Wagner, W.; Stepanenko, V.; Ren, X.; Ogi, S.; Würthner, F. *Angew. Chem. Int. Ed.* **2017**, *56*, 5729.

[12] (a) Kang, Y. T.; Tang, X. Y.; Yu, H. D.; Cai, Z. G.; Huang, Z. H.; Wang, D.; Xu, J. F.; Zhang, X. *Chem. Sci.* **2017**, *8*, 8357; (b) Yang, H.; Ma, Z.; Wang, Z. Q.; Zhang, X. *Polym. Chem.* **2014**, *5*, 1471.

Manuscript received: February 2, 2018
Manuscript revised: March 11, 2018
Manuscript accepted: March 15, 2018
Accepted manuscript online: March 24, 2018
Version of record online: April 19, 2018

